Pergamon

Materials Research Bulletin 36 (2001) 487–496

Materials Research Bulletin

Structural analysis of modified hydroxyapatite powders

M.A. Fanovich, M.S. Castro, J.M. Porto López*

Instituto de Investigaciones en Ciencia y Tecnología de Materiales (INTEMA), (CONICET - Universidad Nacional de Mar del Plata), Av. J.B.Justo 4302 - (7600) Mar del Plata, Argentina

(Refereed)
Received 1 May 2000; accepted 8 September 2000

Abstract

In this work, the presence of structural defects in modified hydroxyapatite (HA) samples were studied. The behavior of HA samples with different chemical compositions was compared. Structural alterations were produced by thermal treatments and high-energy milling. Electron paramagnetic resonance spectroscopy (EPR) was used in order to identify the presence of structural defects. Samples were analyzed at room temperature and the signals observed by electron paramagnetic resonance at $g = 1.999$ were assigned to oxygen vacancies in the apatitic structure. The determination of vacancy concentration ($V_o^{\bullet}$) in each sample was related with the characteristic parameters of the signal and the experimental conditions. XRD and SEM were used as additional characterization techniques. The production and concentration of these vacancies was correlated to the modifications introduced during the processing of the materials. The results were also related with the chemical composition, particle size and crystallinity of the samples.

Keywords: A. Inorganic compounds; C. Electron microscopy; C. X-ray diffraction; D. Defects; D. Electronic paramagnetic resonance

1. Introduction

Several types of natural or synthetic hydroxyapatite [$Ca_{10}(PO_4)_6(OH)_2$, HA] are commercially available not only for use in the biomedical field but also for chromatographic and catalytic applications [1–3]. Despite recent advances in the knowledge of their structure and physicochemical behavior, a number of important aspects still have to be explored, which will help to predict the performance of this material. Rey [4] searched for a relation between

* Corresponding author. Fax: +54-223-4810046.
E-mail address: jmplopez@fi.mdp.edu.ar (J.M. Porto López).

0025-5408/01/$ – see front matter
PII: S0025-5408(01)00526-8

apatite channel and zeolite-like properties based on the structural description made by Beevers and McIntyre. In his work he concluded that the open spaces in the HA structure, which arise from vacant sites, could be involved in the adsorption ability of apatites and their role as catalyst support.

According to its chemical formula, stoichiometric HA should have a Ca/P molar ratio of 1.67. The stability limit of the apatitic structure in HA has been the subject of several studies, covering a rather wide range of compositions [5–7]. The apatitic crystal structure can be preserved with Ca/P ratios as low as 1.5. Therefore, HAs with Ca/P lower than 1.67 are characterized as calcium deficient or non-stoichiometric. Stoichiometric HA is thermally stable up to temperatures near 1400°C. However, when the molar ratio Ca/P is lower than 1.67, HA partially decomposes to β-$Ca_3(PO_4)_2$ (β-TCP) at temperatures above 800°C. In turn, this phase transforms to α-$Ca_3(PO_4)_2$ (α-TCP) at temperatures higher than 1200°C [3]. In diverse structural analyses, the spatial arrangement of atoms and structural units has been described using different experimental techniques, but few of them are specifically sensitive to structural point defects, which may be of great importance in the determination of the physicochemical behavior.

In relation to the description of structural defects, electron paramagnetic resonance spectroscopy (EPR) is used to determine the presence and concentration of oxygen paramagnetic species as oxygen vacancies [8,9]. In ZnO-varistors, oxygen vacancies are detected when the oxygen adsorbed on the sample is desorbed. This process may be interpreted as follows [10]:

$$O^{2-} \Leftrightarrow 1/2O_2 + (V_o) \tag{1}$$

where (V_o) is a neutral oxygen vacancy, containing two electrons to maintain neutrality. The ionization of this new donor center is an easy process, which can be represented:

$$(V_o) \Leftrightarrow (V_o^{\bullet}) + e' \tag{2}$$

This means that a free electron appears in the conduction band, leaving a paramagnetic oxygen vacancy, responsible of the signals detected by EPR. This mechanism may allow the detection of oxygen vacancies in different solids.

Matsumura *et al.* [11], in an EPR study dealing with catalytic activity of stoichiometric and non-stoichiometric HA samples, assigned the paramagnetic signal observed at $g = 1.999$ to the occurrence of oxygen vacancies $(V_o^{\bullet})$ in the HA structure.

Che *et al.* [12] reported that the shape of the signal depends on the structural environment of the paramagnetic species. On the other hand, the intensities of the signals may be evaluated as double integrated intensities, calculated from the empirical relationship [13]:

$$\mathrm{DII} = \frac{I \cdot W^2}{G \cdot m \cdot A \cdot P^2} \tag{3}$$

where I is the signal height, W the signal width, G the gain, m the sample mass, A the modulation amplitude, and P the applied power. Experimentally, the variables appearing in the denominator can be kept constant, and the product $I.W^2$ is used as a comparison parameter between different samples.

Tale 1
Nomenclature of the samples

Sample	Description
C	Commercial HA powder, dried at 80°C.
C-A	C (loose powder) thermally treated 2 h at 1200°C.
C-B	C (compacted) sintered 1 h at 1200°C.
C-I	C mechanochemically treated during 10 h.
C-II	C mechanochemically treated during 20 h.
S	Synthesized HA powder, dried at 80°C.
S-A	S (loose powder) thermally treated 2 h at 1200°C.
S-B	S (compacted) sintered 1 h at 1200°C.
S-I	S mechanochemically treated during 10 h.
S-II	S mechanochemically treated during 20 h.

In this work, EPR spectroscopy was used to study the presence and concentration of oxygen vacancies produced by thermal and mechanochemical treatments in HA samples with different Ca/P ratios. XRD and SEM analyses were used as complementary techniques of characterization.

2. Experimental

2.1. Materials

The starting materials used in this work were non-stoichiometric and stoichiometric HA powders. Commercial HA (Sigma Chem. Co.) containing a molar ratio Ca/P = 1.51 was denoted as C sample. Synthesized HA sample having a Ca/P = 1.67 was obtained by a precipitation method as described elsewhere [14] and denoted as S sample.

2.2. Processing

2.2.1. Thermal treatments

Powders of both starting materials were thermally treated as loose powders during 2 h at 1200°C. In addition, separate samples of the same solids were uniaxially compacted at 15 MPa, sintered at 1200°C during 1 h, and subsequently ground to powder.

2.2.2. Mechanochemical treatments

Initial HA powders were suspended in isopropylic alcohol and treated at 1190 rpm in a planetary mill (Fritsch Pulverisette 7) during 10 and 20 hours. Sintered ZrO_2 bowls (45 ml) and balls (12 mm diameter) were used as a milling media. The complete list of samples prepared is given in Table 1.

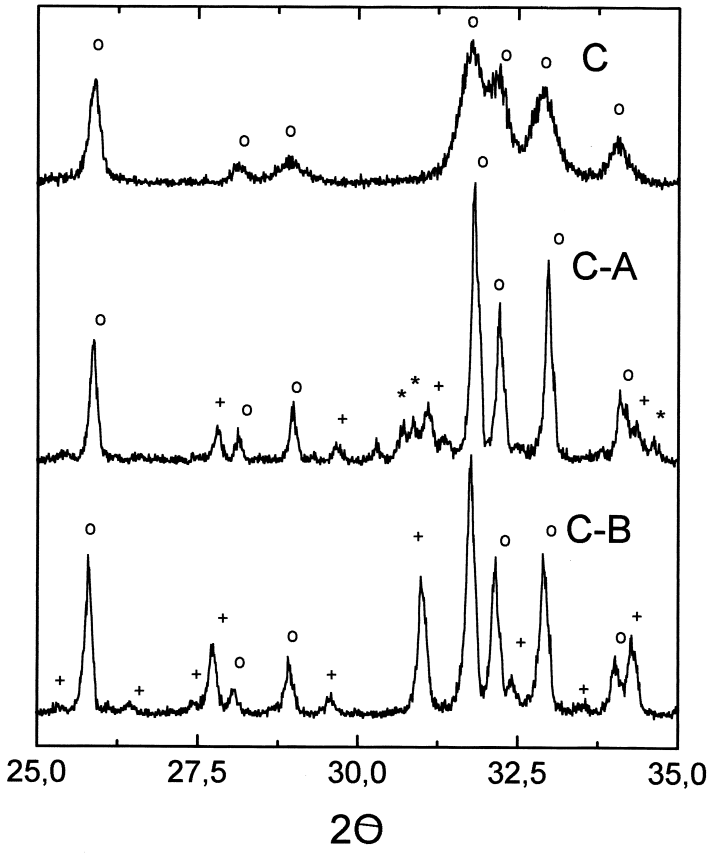

Fig. 1. XRD of samples C, C-A and C-B. (+) β-TCP, (*) α-TCP, (o) HA

2.3. Characterization

The crystalline phases present in the samples were determined by X-ray diffraction (XRD) with a Philips PW 1830 diffractometer, using CuK_{α} radiation and Ni filter, at 40 kV and 30 mA. 250 mg of the treated HA powders were degassed 1 h at 500°C and analyzed by EPR spectroscopy. These analyses were made using a Bruker ER-200D (Band X) spectrometer at a microwave frequency of 9.58 GHz, a microwave power of 5 dB, and a modulator frequency of 100 KHz. Microstructural and morphological characterization was performed on powdered samples with a Philips 505 SEM.

3. Results and discussion

3.1. Effect of thermal treatment

The commercial HA (C sample) consisted in poorly crystalline HA. This sample decomposed into stoichiometric HA and β-TCP when treated during 2 h at 1200°C (C-A sample)

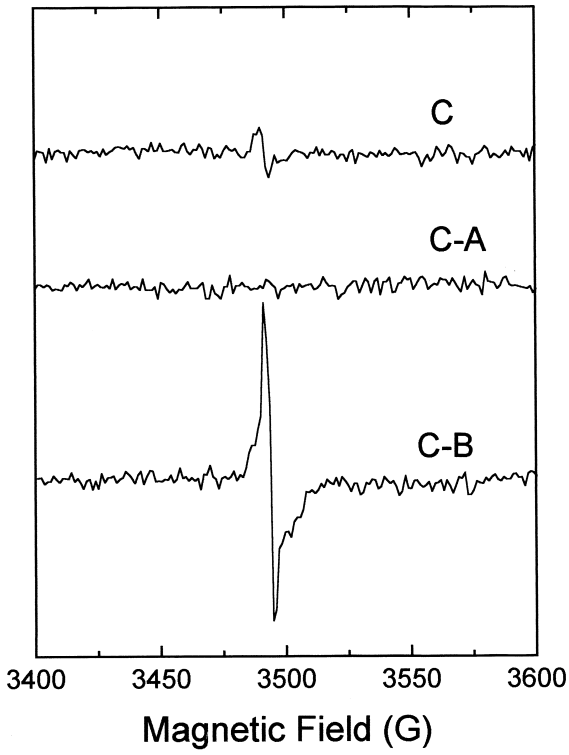

Fig. 2. EPR spectra of samples C, C-A and C-B.

because to its non-stoichiometry [15]. The XRD diffractograms of these samples are shown in Fig. 1. β-TCP peaks were clearly noted in samples C-A and C-B but not in sample C. On the other hand, the EPR analyses showed additional differences between the C, C-A and C-B samples (Fig. 2, and Table 2). Sample C showed a relatively low signal due to oxygen vacancies ($V_o^{\bullet}$). However, when this sample was thermally treated (C-A sample) no signal was detected. This observation suggests that the thermal treatment produce a reduction in the ($V_o^{\bullet}$) concentration when the sample is treated as a loose powder.

On the other hand, the intensity in the EPR signal for C-B sample (C sample thermally treated as compacted powder) increased with respect to the corresponding signal for C sample. In this case, during the densification process, dehydroxylation and loss of adsorbed oxygen is produced [16]. In such an environment, in which extensive pore closure occurs, the oxygen uptake is very difficult, and the oxygen vacancies previously created cannot be easily

Table 2
W^2I values determined from EPR signals at g = 1.999

Sample	C	C-A	C-B	C-I	C-II	S	S-A	S-B	S-I	S-II
$W^2.I$	1.8	nd	7.2	36.9	>50	nd	nd	nd	2.1	4.3

nd: no signal detected.

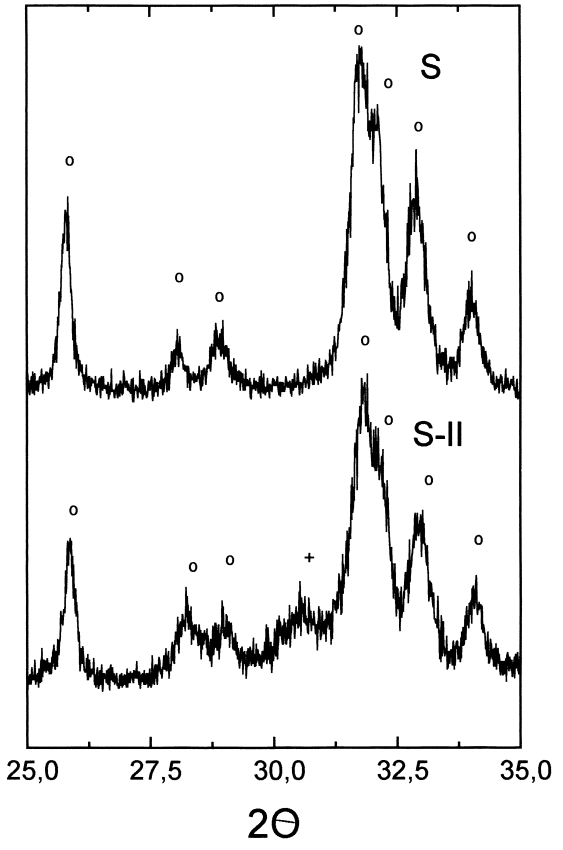

Fig. 3. XRD of samples S and S-II. (+) β-TCP, (o) HA

annihilated by atmospheric oxygen during cooling. This behavior may be also related with the formation of α-TCP and β-TCP in these samples. For this reason, although the temperature of treatment was the same for C-A and C-B, the different processes confirm the impossibility of oxygen uptake by sintered samples, which is not the case in those thermally treated as loose powders. This fact could justify the absence of oxygen vacancies in C-A.

Moreover, sample S (stoichiometric) was found to be stable up to 1200°C; only HA phase was detected by XRD. Secondary phases were neither detected by XRD analyses after thermal treatment. The S, S-A and S-B samples did not show the presence of oxygen vacancies by EPR analysis (see Table 2).

3.2. Effect of mechanochemical treatment

Significant changes were detected in the XRD diffractograms when sample S was mechanochemically treated. Fig. 3 shows the presence of HA phase in the sample S and the presence of HA and β-TCP in sample S-II, along with the loss in intensity of the diffraction peaks corresponding to HA. The same behavior was observed for sample C. It is known that the use of high-energy milling produces the reduction in the particle size, but in addition the

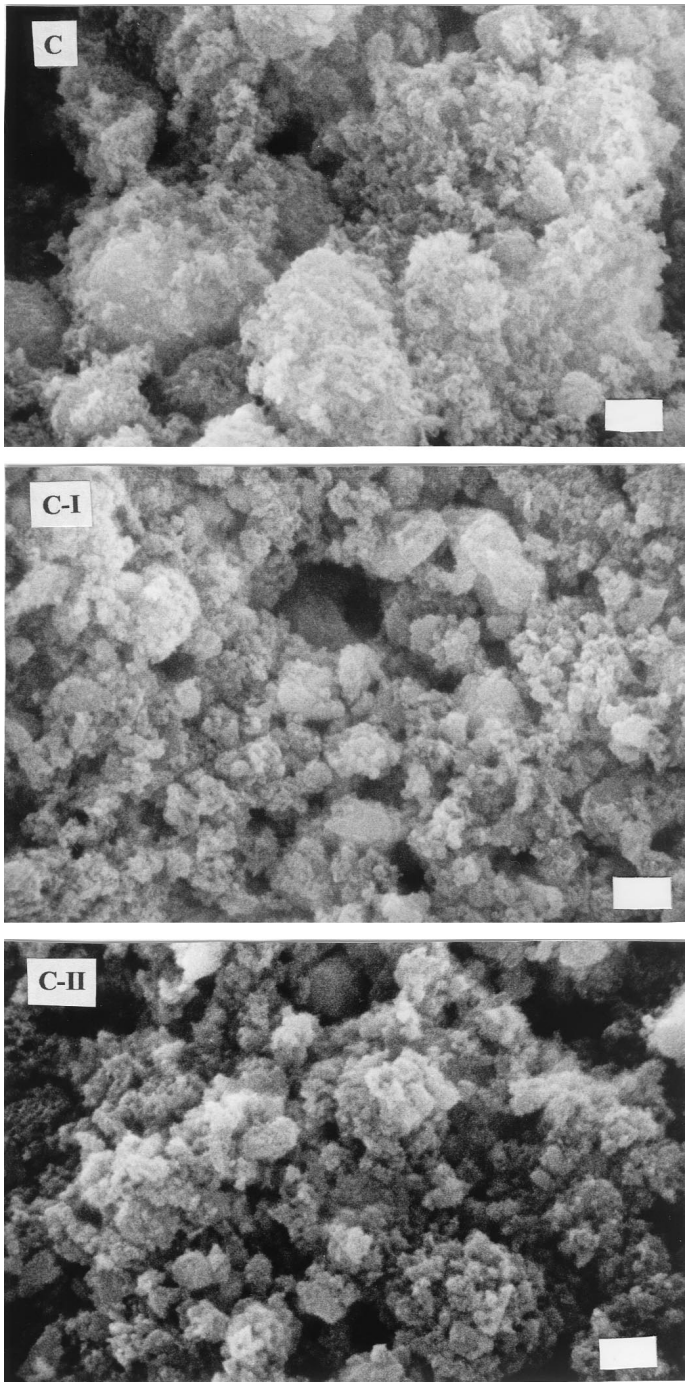

Fig. 4. SEM micrograph of HA powders before and after different times of mechanochemical treatment. Bar = 1 μm.

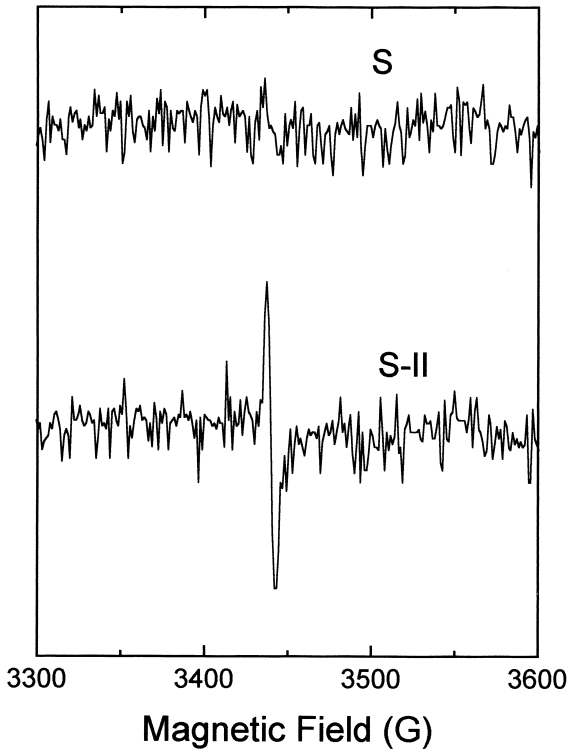

Fig. 5. EPR spectra of samples S and S-II.

impact and friction effects lead to structural changes associated with the amorphyzation of the crystal lattice [17].

Fig. 4 shows the SEM micrographs of powdered samples C, C-I, and C-II. S series showed a similar behavior. It was observed a decrease in particle size in the samples treated during 10 h, while in the samples S-II and C-II the apparent size increased, due to the extensive agglomeration of the activated particles. Simultaneously, a progressive loss of the original crystalline morphology occurred, resulting in particles with irregular surfaces and rounded edges. These observations agree with the interpretation of the mechanochemical treatment as a progressive deterioration of the original crystalline structure, with production of extended defects and, in some samples, partial decomposition of the solid. Moreover, these observations are in accordance with the XRD measurements, in which a loss of crystalline order was evidenced through the reduction of the integrated intensity of the peaks assigned to HA phase.

On the other hand, the sample S did not presented ($V_o^{\bullet}$) signal by EPR analysis as was mentioned above. However, as the time of mechanochemical treated was increased, the oxygen vacancies amount increased. This effect is shown in Fig. 5 and related with the values of ($V_o^{\bullet}$) concentration in Table 2. Sample S-II presented a strong signal due to ($V_o^{\bullet}$) whereas the sample S-I, presenting a signal due to ($V_o^{\bullet}$), showed one of lower intensity (Table 2). To explain this changes in ($V_o^{\bullet}$) concentration for S, S-I and S-II, it is necessary to take into

account the structural changes introduced by the processing. The mechanochemical process can be interpreted to proceed through two steps that cannot be separated. The production of textural changes which can be detected by microscopy examination, and the alteration in chemical-structural properties of the material. Although both steps occur simultaneously, the later effect arises from the formation of particles containing high superficial energy. This process is distinguished of a thermal process, since the influence of temperature variations occurs in the totality of the solid mass, while that a mechanochemical process produces energetic alterations in restricted surface regions of the solid. The materials obtained by this process do not have similar properties with those made by thermal methods [18,19]. On the contrary, the stresses created in the solid are enough to modify its structure and to lower the internal order. As a result of this process, the production of defects and the loss in crystallinity bring along an increase in the oxygen vacancy concentration.

Additionally, for C sample a substantial signal of ($V_o^{\bullet}$) was observed, which increased in intensity for C-I and C-II samples (Table 2). This behavior is a consequence of the mechanochemical process, and is also related to the Ca-defective structure of C sample.

4. Conclusions

HA samples with different ($V_o^{\bullet}$) concentration could be obtained by thermal or mechanochemical treatments. Thermal treatments on Ca-deficient HA produce a decrease in ($V_o^{\bullet}$) simultaneously with decomposition into stoichiometric HA and β-TCP. However, thermal treatments on compacted powder did not result in extensive defect healing, because of the high densification achieved, which hindered the oxygen uptake.

Mechanochemical treatments produced an increase in oxygen vacancy concentration in all the samples. However, for stoichiometric HA samples this variation was evidenced only at longer treatment times. It was determined that this type of treatment introduces crystalline disorder in the structures with formation of secondary phases.

As previously stated, the importance of EPR spectroscopy in this work lies on the possibility of identification of structural defects. In this way, the use of HA materials as substrate with specific adsorption properties or catalytic activity could be assessed through the control of ($V_o^{\bullet}$) concentration by EPR analyses.

Acknowledgments

The authors are grateful to Dr. L. Perissinotti (Mar del Plata University) for the determinations of the EPR spectra. In addition, the authors M.A.F. and J.M.P.L. acknowledge partial support for this study, given by Project CYTED VIII.6, and by the Third World Network of Scientific Organizations (TWNSO) through JRP 18/95.

References

[1] H. Aoki, Medical Applications of Hydroxyapatite, Ishiyaku EuroAmerica, Tokyo, 1994.
[2] Y. Matsumura, J.B. Moffat, J. Catal. 148 (1994) 323.
[3] A. Ravaglioli, A. Krajewski, Bioceramics Chapman and Hall, London, 1992.
[4] C. Rey, in Hydroxyapatite and Related Materials, eds. Brown P.W., B. Constantz, p. 257, CRC Press, Inc., 1994.
[5] P.E. Wang, T.K. Chaki, J. Mater. Sci.: Mat. in Med. 4 (1993) 150.
[6] K. De Groot, C.P.A. Klein, J.G.C. Wolke, J.M.A. De Blieck-Hogervorst, in Handbook of bioactive Ceramics, eds. T. Yamamuro, L.L. Hench, J. Wilson, Vol. II, CRC Press, Boca Raton, FL, 1990.
[7] H.Y. Juang, M.H. Hon, Biomaterials 17 (1996) 2059.
[8] M.S. Castro, C.M. Aldao, J. Eur. Ceram. Soc. 18 (1998) 2233.
[9] S. Ezhilvalavan, T.R.N. Kutty, J. Mat. Sci.: Mat. Electron. 7 (1996) 137.
[10] F. Morazzoni, R. Scotti, S. Volontè, J. Chem. Soc. Faraday Trans. 86 (1990) 1587.
[11] Y. Matsumura, H. Kanai, J.B. Moffat, J. Molec. Cat. A.: Chem. 115 (1997) L229.
[12] M. Che, A.J. Tench, Advances in Catalysis 31 (1982) 77.
[13] N.S. Hari, T.R.N. Kutty, J. Mat. Sci. 33 (1998) 3275.
[14] M.A. Fanovich, J.M. Porto López, J. Mater. Sci. Mater. in Medicine 9 (1998) 53–60.
[15] A. Slósarczyk, E. Stobierska, Z. Paszkiewicz, M. Gawlicki, J. Am. Ceram. Soc. 79 (1996) 2536.
[16] L.L. Hench, in Handbook of Bioactive Ceramics, eds. T. Yamamuro, L.L. Hench, J. Wilson, Vol. 1, CRC Press, Boca Raton, 1990.
[17] A.N. Scian, E.F. Aglietti, J.M. Porto López, E. Pereira, Rev. Lat. Am. Ing. Quím. Apl. 14 (1984) 51.
[18] E.M. Gutman, Mechanochemistry of Materials, Cambridge Internat. Sci. Publ. (1998).
[19] V. Boldyrev, A. Avvakumov, Russian Chem. Rev. 40 (1971) 847.